



**HAL**  
open science

## High speed electromechanical response of ionic microactuators

Ali Maziz, Cedric Plesse, Caroline Soyer, Eric Cattan, Frédéric Vidal

► **To cite this version:**

Ali Maziz, Cedric Plesse, Caroline Soyer, Eric Cattan, Frédéric Vidal. High speed electromechanical response of ionic microactuators. Conference on Electroactive Polymer Actuators and Devices (EAPAD) 2015, Mar 2015, San Diego, United States. pp.1-8, 10.1117/12.2085516 . hal-03280237

**HAL Id: hal-03280237**

**<https://uphf.hal.science/hal-03280237>**

Submitted on 4 Jul 2022

**HAL** is a multi-disciplinary open access archive for the deposit and dissemination of scientific research documents, whether they are published or not. The documents may come from teaching and research institutions in France or abroad, or from public or private research centers.

L'archive ouverte pluridisciplinaire **HAL**, est destinée au dépôt et à la diffusion de documents scientifiques de niveau recherche, publiés ou non, émanant des établissements d'enseignement et de recherche français ou étrangers, des laboratoires publics ou privés.



Distributed under a Creative Commons Attribution 4.0 International License

# High speed electromechanical response of ionic microactuators

Ali Maziz<sup>a</sup>, Cedric Plesse<sup>a</sup>, Caroline Soyer<sup>b</sup>, Eric Cattan<sup>b</sup>, and Frederic Vidal<sup>a</sup>

<sup>a</sup> LPPI – EA2528, Institut des Matériaux, 5 mail Gay Lussac, Neuville sur Oise, 95031 Cergy-Pontoise cedex, France, <sup>b</sup> IEMN, UMR-8520, Université de Valenciennes, Le Mont Houy, 59313 Valenciennes cedex 9, France

## ABSTRACT

This paper presents the synthesis and characterization of thin and ultra-fast conducting polymer microactuators which can operate in the open air. Compared to all previous existing electronic conducting polymer based microactuators, this approach deals with the synthesis of robust interpenetrating polymer networks (IPNs) combined with a spincoating technique in order to tune and drastically reduce the thickness of conducting IPN microactuators using a so-called “trilayer” configuration. Patterning of electroactive materials has been performed with existing technologies, such as standard photolithography and dry etching. The smallest air-operating microbeam actuator based on conducting polymer is then described with dimensions as low as  $160 \times 30 \times 6 \mu\text{m}^3$ . Under electrical stimulation the translations of small ion motion into bending deformations are used as tools to demonstrate that small ion vibrations can still occur at frequency as several hundreds of Hz. Conducting IPN microactuators are then promising candidates to develop new MEMS combining downscaling, softness, low driving voltage, and fast response speed.

**Keywords:** conducting IPNs, PEDOT, microactuators, microsystems, fast ionic motion

## 1. INTRODUCTION

Electronic conducting polymers (ECPs) are now considered as a very important class of materials which exhibit interesting electrical and optical properties [1]. They have also attracted considerable attention because of potential dimensional changes generated by the ion expulsion/inclusion motions during oxidation and reduction processes [2–5]. As a result, ECPs might be used as the active material in actuators for interesting applications such as robotics, prosthetics and micro-valves [2]. Actuators designed for operation in open air are usually built as three-layer system with an internal layer composed of a solid polymer electrolyte (SPE) sandwiched between two ECP layers (ECP//SPE//ECP). The relative differential expansion between conducting polymer layers results in bending [2].

In those systems, the diffusion phenomena of ions and solvents into the ECP is a rate-limiting step in the actuation performances as with every ionic EAP [6], making them considered to be slow devices, typically in the range of 1 Hz which is not sufficient for many applications. In order to increase speed, the ionic conductivity has to be increased and/or the distance between electroactive layers has to be reduced. The miniaturization of tri-layer actuators operating in air has been described using a laser ablation technique [7] or a combination of photolithography and reactive ion etching (RIE) [8] for fabricating sub-millimeter sized devices. In such system the SPE layer plays a key role in the ultimate performances of these electrochemomechanical devices and the decrease of its thickness is the main limiting factor hindering further miniaturization of the conducting polymer actuators operating in air. Indeed, they have to provide suitable mechanical properties while keeping ionic conductivity as high as possible. This drawback has been recently solved by the synthesis of ultrathin conducting interpenetrating polymer network (IPN) microactuators using the spincoating method and patterning through microsystem techniques. The SPE is synthesized as an IPN based on a PEO network for ionic conductivity with improvement of mechanical properties by the interpenetration of a high molecular mass elastomer, nitrile butadiene rubber (NBR), within the PEO network. After interpenetration of two poly(3,4-ethylenedioxythiophene) (PEDOT) electrodes and incorporation of an ionic liquid as electrolyte, large displacements under  $\pm 4\text{V}$  above 900 Hz corresponding to the fundamental eigenfrequency have then been demonstrated for a  $690 \times 45 \times 12 \mu\text{m}^3$  microbeam actuator [9].

In the present work, the smallest air-operating microbeams actuator based on ECP will be described ( $160 \times 30 \times 6 \mu\text{m}^3$ ). The synthesis of  $6 \mu\text{m}$  thick SPE will be presented as well as the interpenetration of PEDOT electroactive electrodes. Patterning of this pseudo-trilayer structure will be discussed as a function of the chemical nature of the polymer partners. Finally electromechanical response under electrical stimulation will be presented.

## 2. EXPERIMENTAL SECTION

**Synthesis of Poly(ethylene oxide)/nitrile butadiene rubber thin film.** PEO/NBR 50/50 IPN films are obtained by an in-situ polymerization according to a modified method of previously described procedure [9,10,11]. First the linear NBR solution is prepared by dissolving NBR in cyclohexanone (1:5 weight ratio). After complete dissolution, DCP (6 wt% vs NBR) as cross-linker was then added to the mixture. PEO network precursors (50 wt% vs NBR) are introduced by adding PEGM monomer (75 wt% of the PEO network) and PEGDM crosslinker (25 wt% of the PEO network). DCPD initiator (3 wt% PEO precursors) was then introduced and the mixture was stirred for 30 min under vacuum. When homogenization was achieved, aqueous PVA solution at 300 g.L<sup>-1</sup> was firstly spincoated onto a glass slide (3000 rpm, 3000 rpm.s<sup>-1</sup> for 30 s, corresponding to 2.2 μm thick layer) and dried at 80°C. Afterwards, the homogeneous mixture of PEO and NBR was spincoated. The thickness of the polymer films depends on the selected spinner speed, time and solution viscosity. The substrate is then kept at 50°C for 4 h and then postcured for 2 h at 80°C. The temperature is then increased for 60 min at 160°C for the crosslinking step of NBR. The lift-off of the PEO/NBR IPN is carried out in water by dissolving the PVA sacrificial layer. The resulting PEO/NBR IPNs were then dried 4 h at 70°C under vacuum. Freestanding PEO/NBR IPNs are thus obtained.

**Trilayer actuators preparation.** The methodology for the preparation of conducting IPN actuators has been described previously [9]. IPN films are swollen with EDOT vapor under reduced pressure for given lengths of time. The swollen films were then immersed in an iron III trichloride FeCl<sub>3</sub> aqueous oxidative solution (1.5 mol.L<sup>-1</sup>) for an oxidative polymerization of EDOT. This synthetic pathway ensures a non-homogeneous distribution of the electronic conducting polymer throughout the thickness of the PEO/NBR IPN. After polymerization, the resulting films were washed with methanol, i.e. excess of FeCl<sub>3</sub> is removed, and dried under vacuum at 40°C for 1 h. The edges of the thin film were then trimmed off. The chemical synthesis was optimized to avoid short circuit between the two ECP electrodes. Very thin C-IPN films of 3.5 to 14 μm are obtained. Prior to electrochemomechanical characterization, the actuators were immersed in EMITFSI for at least 72 hours until saturation.

**Microactuators patterning process.** Patterning using standard photolithography and a dry etching technique were carried out according to a procedure described elsewhere [8,9]. Firstly, C-IPN films were fixed on silicon substrates with a PVA adhesive layer (from a spincoated aqueous solution at 1500 rpm/750 rpm.s<sup>-1</sup> for 15s, 5 μm thick layer was obtained). The positive photoresist SPR220-7μm (Microchem Corporation) is spincoated at 1000 rpm for 40s, with a ramp rate of 750 rpm.s<sup>-1</sup>. The softbake for SPR220 was 115°C on a contact hotplate with slow ramp up and down to avoid formation of cracks. The resulting ~ 17 μm thick photoresist is then patterned. Photoresist was exposed through a mask to an energy dose of 400 mJ.cm<sup>-2</sup> during 40 s with a light at 365 nm. A hold time of at least 180 min is required to complete the photoreaction before the next step. The sample is then soaked in the corresponding photoresist developer (Microchem Corporation MF-326) for 10 min in order to obtain a patterned protective layer on top of the C-IPN. In a second step, dry etching of C-IPN was achieved using reactive ion etching. The C-IPN actuators were etched with a mixture of O<sub>2</sub>/CF<sub>4</sub> gas (90/10) at 300 W and 200 mT. Finally, the remaining photoresist is removed with acetone and the C-IPN lift-off was carried out by dissolution of PVA sacrificial layer in water. Ionic liquid incorporation was then performed producing self-standing microactuators.

**Electrochemomechanical characterizations.** The frequency-dependent tip displacements of the microactuators were measured using a laser displacement sensor (Keyence laser LK-G32). From the resulting displacement signal, strain difference between the electrodes was calculated according to Sugino et al. [12]:

$$\Delta\varepsilon = \frac{2Dh}{L^2 + D^2} \quad (1)$$

Where  $\Delta\varepsilon$  is the strain difference, D is half of the peak to peak displacement, h is the thickness of the actuator (measured with SEM microscope after swelling in electrolyte), and L is the distance from the clamped end of the actuator to the projection of the laser.

The output force was measured using a FT-S Microforce Sensing Probes from FemtoTools. Microforce sensors are capable of measuring forces from millinewtons (10<sup>-3</sup> N) down to several nanonewtons (10<sup>-9</sup> N) along the sensors' probe axis. Both compression and tension forces can be measured. The measured force is calculated by the equation  $F = \text{Sensor}$

Gain \* (Vout - Vout,0) / F, where F is the force axially applied to the sensor probe, Vout,0 is the output voltage at zero load and Vout is the output voltage as the load is applied. A tensile force will result in an increase of the output voltage whereas a compression force will result in a decrease of the output voltage. Each individual sensor is delivered with calibration data sheet.

### 3. RESULTS AND DISCUSSION

#### 3.1 Synthesis of the pseudo-trilayer conducting IPNs

Figure 1 summarizes the general procedure to obtain ultrathin conducting IPN presenting a pseudo-trilayer configuration. The central SPE is synthesized first. The ideal SPE matrix must (i) be polar so as to swell in various electrolyte media, (ii) offer sufficient free-volume in order to improve the ions mobility in the membrane, and (iii) present good damping properties in order to prevent crack formation during actuation or integration. Herein, the polarity of the material can be obtained by the use of polyethylene oxide (PEO) networks which is a classical SPE despite usually poor mechanical properties. Free-volume can be provided through the synthesis of PEO networks with dangling chains [10-11,13-14]. In order to improve the resulting mechanical properties, IPN architecture can be a powerful approach by combining a second network in the first one as continuous phases. In this study a high molecular weight elastomer (NBR) will ensure convenient mechanical properties.

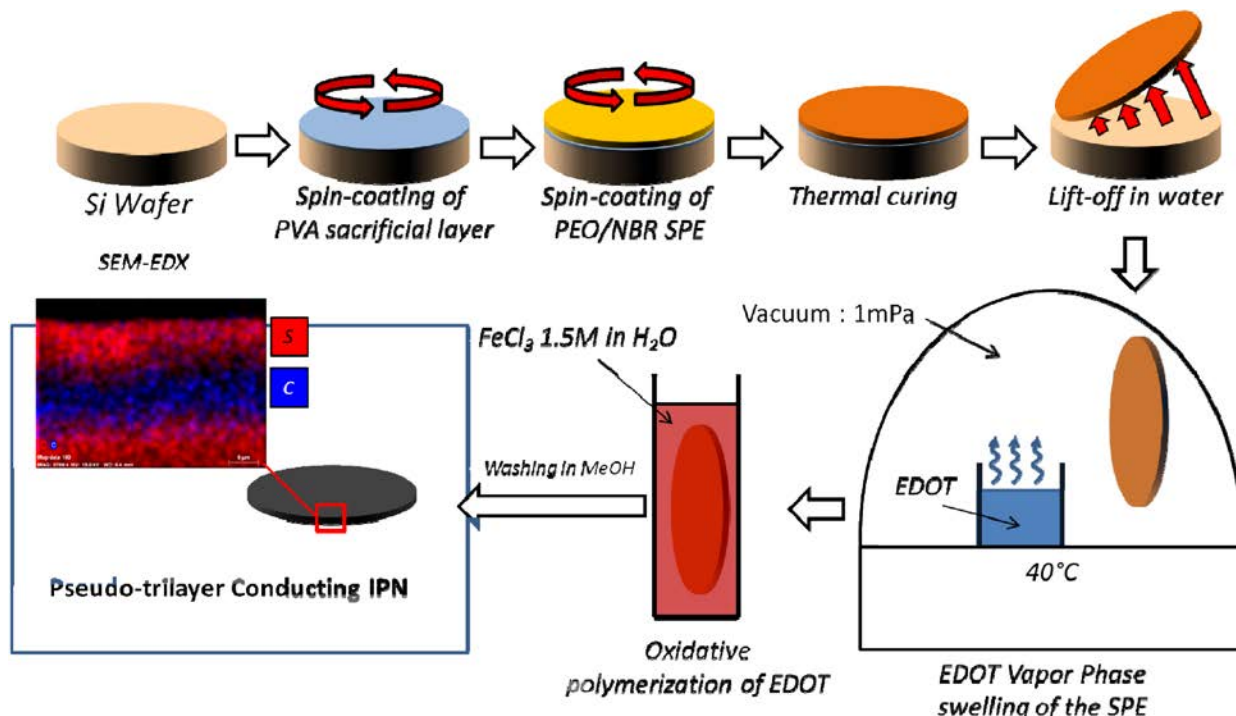


Figure 1:

PEO/NBR IPNs are obtained following an *in-situ* pathway with sequential polymerization. All the SPE precursors are solubilized in cyclohexanone, a high boiling point solvent. The reactive mixture is then applied by spin-coating on a Si wafer coated with a PVA underlayer. The resulting thin viscous layer is thermally cured under inert atmosphere. The PEO network is obtained first at 50°C by free radical copolymerization of PEGM (monomer) and PEGDM (acting as crosslinker) initiated by DCPD. Raising the temperature to 160°C, NBR is then cross-linked in the presence of the PEO network by DCP. After solubilization of the PVA underlayer in water, the IPNs are released as thin membranes that can be manipulated many times without suffering from cracking. PEO/NBR SPE can be obtained with tunable thicknesses from 30 μm to 600 nm with very good reproducibility.

In a second step conducting IPN were prepared according to the procedure described elsewhere [9,10]. Typically, EDOT monomer is incorporated into the SPE by gas-phase swelling under reduced pressure until the swelling ratio reached the desired value of 150% of the initial SPE mass. Next, samples were dipped for different length of time into an aqueous iron III trichloride ( $\text{FeCl}_3$ ) solution at 40 °C for the oxidative chemical polymerization of EDOT. Water is chosen as the solvent for the oxidative polymerization of EDOT due to the low EDOT solubility in water, i.e.  $1.5 \cdot 10^{-2} \text{ mol L}^{-1}$ . The polymerization rate and the diffusion of EDOT out of the film into the aqueous solution is slow and allows the penetration of  $\text{FeCl}_3$  in the matrix before a significant amount of EDOT leaves the matrix. This synthetic pathway ensures a non-homogeneous distribution of the ECP throughout the thickness of the PEO/NBR IPN: two PEDOT layers are then interpenetrated into the both faces of the SPE leading to the desired pseudo-trilayer configuration. Three different thicknesses have been obtained: 3.5, 8 and 14  $\mu\text{m}$ . The electrolyte necessary to the redox process of the conducting polymer is subsequently introduced in the electroactive material through a swelling step. The chosen electrolyte is the ionic liquid  $\text{N,N}'$ -ethylmethylimidazolium bis(trifluoromethylsulfonyl)imide (EMITFSI). After the swelling step the total thickness of the samples is increasing to 6, 12 and 19  $\mu\text{m}$ .

Then the samples can be macroscopically dimensioned with scissors or microsized using photolithography and reactive ion etching. In both cases microbeam geometries have been chosen since mechanical models are well established.

### 3.2 Determination of the Young modulus of macroscopic bending beam actuators

The Young modulus of the beams has been measured on macroscopic samples according to two approaches. First the Young modulus has been estimated by measuring the resonant frequency of 19 $\mu\text{m}$  thick beams with different free lengths  $L$  ranging from 2.5 cm to 4 mm (Figure 2A and 2B) under +/-3V electrical stimulation. Resonant frequencies ranging from 6.4 to 60 Hz have been obtained respectively and are increasing linearly with  $1/L^2$ . According to equation (2) the Young modulus of the macrobeams has been estimated to be 178 MPa which is in the range of previous values [9].

$$f_n = \frac{1}{2\pi\sqrt{12}} \alpha_n^2 \frac{h}{L^2} \sqrt{\frac{E}{\rho}} \quad (2)$$

Where  $\alpha_n$  is the resonant frequency mode (1.875 for fundamental resonant frequency) and  $\rho$  is the mass density (1700  $\text{kg/m}^3$ ).

The Young modulus has been also determined using the Hooke's law. A displacement is applied to the macrobeam ( $L=2.5\text{mm}$ , width= $0.75\text{mm}$ , thickness= $19\mu\text{m}$ ) with a sensor probe and the resulting force is measured. The stiffness of the beam is then used to calculate the Young modulus according to equation (3):

$$E = \frac{12kL^3}{3wh^3} \quad (3)$$

Where  $k$  is the stiffness of the beam,  $L$  the length,  $w$  the width and  $h$  the thickness. A Young modulus of 170 MPa is obtained. Then the two methods provide similar values for the microbeam modulus.

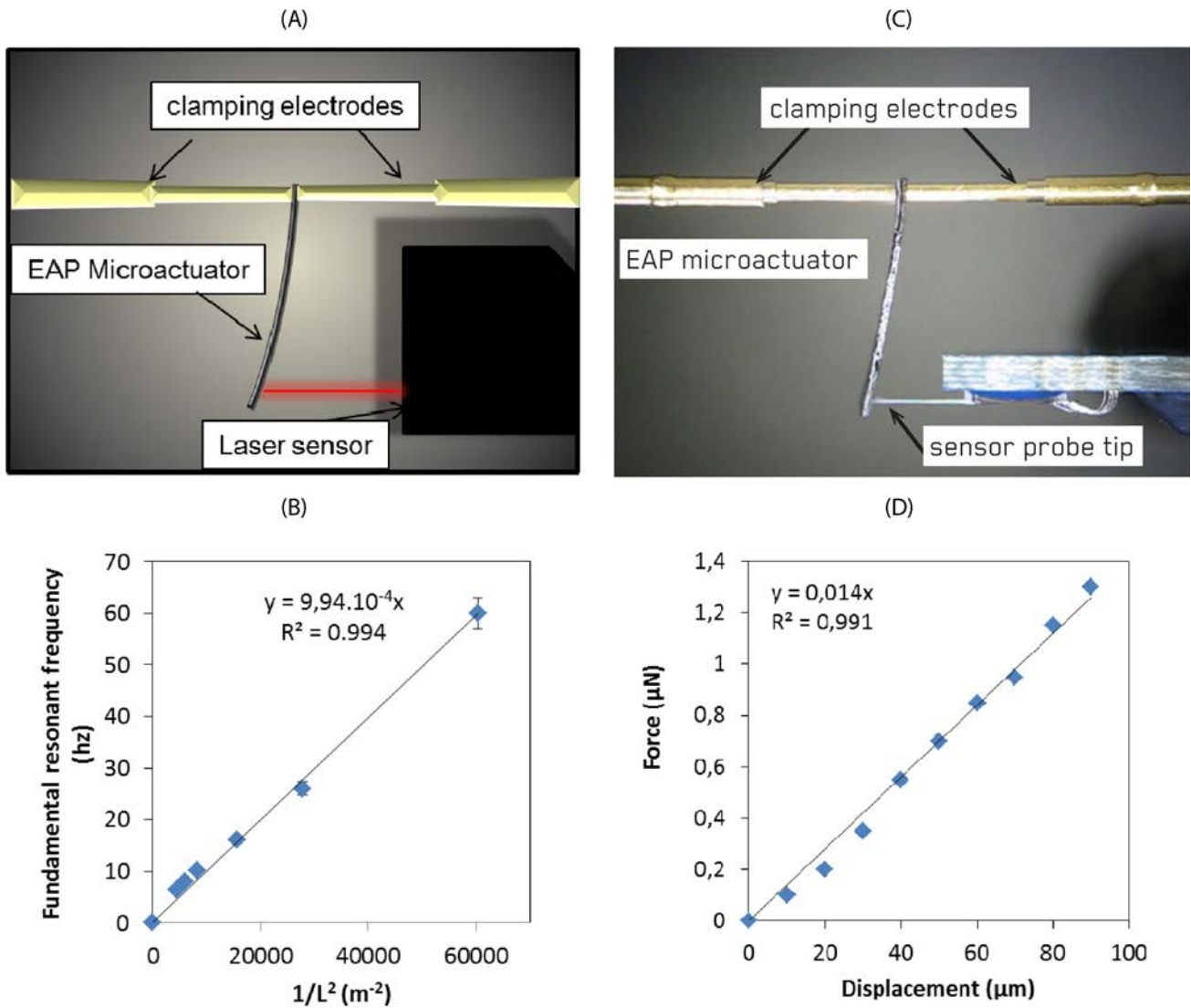


Figure 2: (A) Scheme of the experimental setup for Young modulus measurement using the resonant frequency of the beams (B) Fundamental resonant frequency of 19µm thick macrobeam actuators as a function of  $1/L^2$  under electrical stimulation of +/- 3V. Actuator dimensions. Width= 0.75 mm. (C) Photograph of the experimental setup for Young modulus measurement using Hooke's law. (D) Measured force as a function of displacement imposed by sensor probe tip. Actuator dimensions Length=2.5 mm, width= 0.75 mm, thickness= 19 µm.

### 3.3 Patterning of pseudo-trilayer conducting IPNs into microbeam actuator

The ultrathin conducting IPN are then patterned into microbeam actuators using photolithographic methods. The materials are etched using reactive ion etching (RIE) in a 90/10 O<sub>2</sub> / CF<sub>4</sub> plasma at 300 W and 200 mT. The RIE was performed without prior EMITFSI swelling of the conducting IPN. Table 1 summarizes the etching rates of the conducting IPNs (thickness 3.5, 6 and 14µm), the PEO/NBR IPN and each individual component. Etching rates are also compared with the one of the Megaposit SPR 220 7.0 photoresist that will be used to protect the actuator locally during the dry etching.

Table 1. Etching rate and selectivity of conducting IPN, IPN and individual components in a O<sub>2</sub>/CF<sub>4</sub> (90/10) plasma, 300W, 200 mTorr.

Material	Nature	Etching time (min)	Etching rate (μm/min)	Selectivity <sup>a</sup>
PEO-NBR-PEDOT 14 μm	conducting IPN	5	1.05	1.5
PEO-NBR-PEDOT 8 μm	conducting IPN	5	0.85	1.2
PEO-NBR-PEDOT 3.5 μm	conducting IPN	5	0.8	1.15
PEO-NBR	IPN	5	0.4	0.6
PEO	saturated polymer	4	1	1.4
NBR	unsaturated polymer	4	0.5	0.7
PEDOT	conjugated polymer	/	n.m. <sup>b</sup>	n.m. <sup>b</sup>

<sup>a</sup> ratio between the etching rate of the material and the etching rate of the Megaposit SPR 220 7.0 photoresist in the O<sub>2</sub>/CF<sub>4</sub> (90/10) plasma at 300W, 200 mTorr

<sup>b</sup> non-measurable

Etching rate of the PEO single network and NBR single network are 1 μm/min and 0.5μm/min respectively. However no etching step can be measured for PEDOT in these conditions as it has been described previously. The PEO/NBR IPN presents an etching rate around 0.4 μm/min, close to the one of the rubber network. This result can be explained by the continuity of the NBR network in the whole SPE, then being the limiting factor of the etching process. Interestingly PEO/NBR/PEDOT conducting IPNs present etching rate higher than those of individual components. Etching rate is ranging between 0.8 and 1.05 μm/min for the three different thicknesses of the electroactive materials. This behavior has already been described previously [8] and has been attributed to a “self-degradation” process in the presence of PEO and PEDOT.

In these conditions selectivities ranging from 1.15 to 1.5 are obtained, indicating that the Megaposit SPR 220 7.0 photoresist was etched more slowly than the actuator. As a consequence the conducting IPNs can be fully patterned before the protective photoresist layer is fully etched. Then microfabrication of conducting IPN microactuators can be performed with precise control of the geometry for the three different thicknesses.

### 3.4 Actuation of the conducting IPN microactuator

To turn microbeam into microactuator EMITFSI ionic liquid is incorporated through a swelling step of the material. As illustrated on figure 3 the microbeam actuator as small as 160x30x6μm<sup>3</sup> can be obtained which is to the best of our knowledge the smallest air-operating microbeam actuator based on ECP.

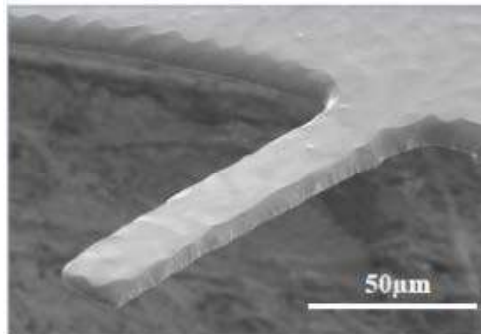


Figure 3: SEM micrograph of conducting IPN microbeam (160x30x6 μm<sup>3</sup>)

Microbeam actuators are then stimulated electrically with square wave potential ( $\pm 2V$ ) at frequencies ranging from 1Hz to 500Hz. Interestingly, the actuator deformation remains almost constant (90% of the initial amplitude at 1Hz) up to 50 Hz indicating that full actuation is available up to this frequency. Since the actuation at low frequency is mainly ruled by the redox process in the conducting polymer actuators [3], it can be concluded that complete oxidation/reduction of the conducting polymer electrodes occurs. Then the synthesis of ultrathin SPE allows a drastic decrease of diffusion distances and then promotes fast actuation speed. The maximum strain difference at 1 Hz is equal to 1.13% corresponding to a peak-to-peak displacement of 50  $\mu m$ . For frequencies higher than 50Hz, the strain difference decreases indicating that less and less PEDOT is undergoing redox process. At 500Hz the strain difference is equal to 0.25% corresponding to a peak-to-peak displacement of 10.3  $\mu m$ .

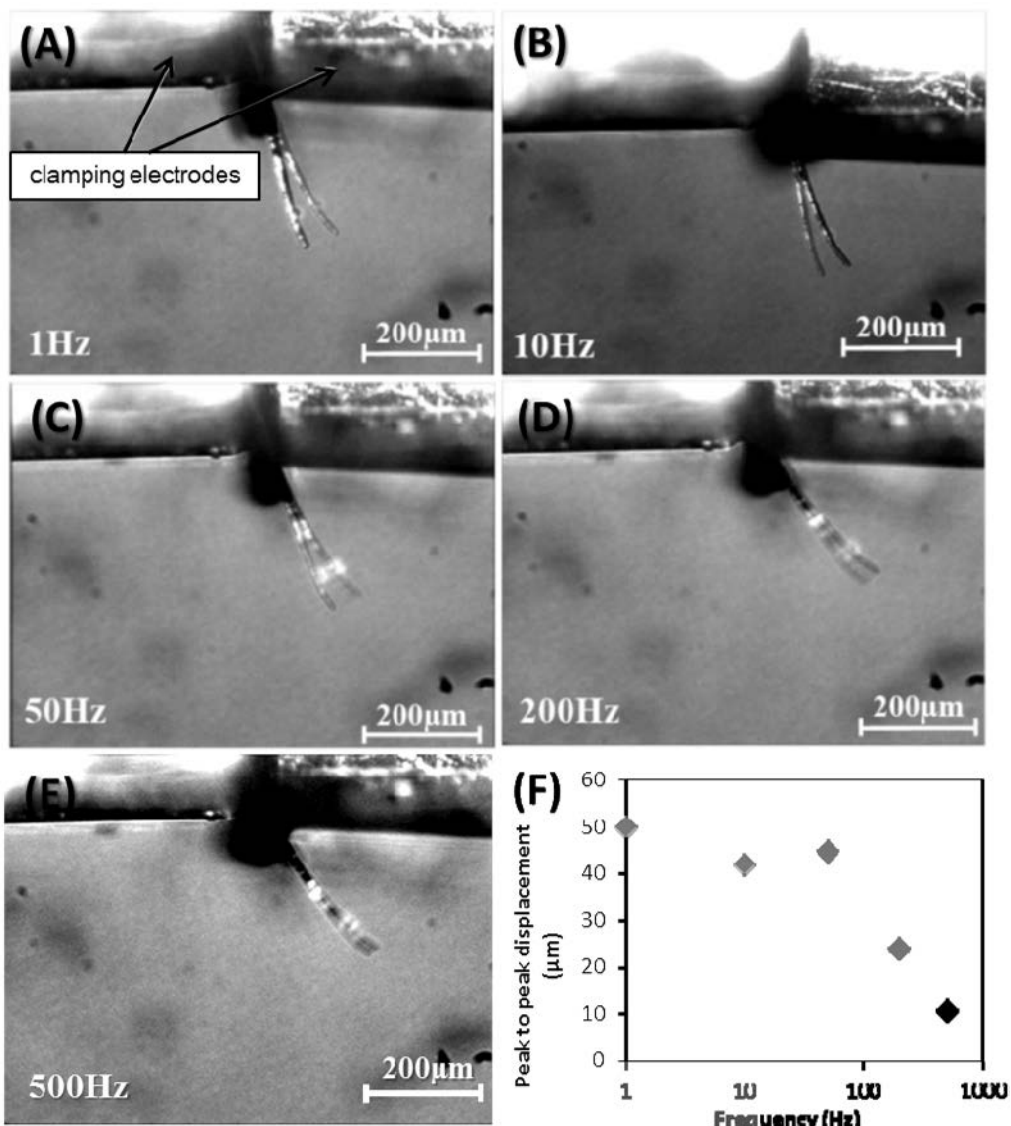


Figure 4: (A) to (E) photograph of microbeam actuator ( $160 \times 30 \times 6 \mu m^3$ ) stimulated in open-air with  $\pm 2V$  square wave potential. (F) Peak-to-peak displacement measured at  $L=160 \mu m$  as a function of the frequency

At 500 Hz, the microactuator still presents a small strain difference of 0.2%. While it is difficult to conclude about the share of the redox process in the actuation response at this rate, it can be supposed that small movements of ions are still involved in actuation at such frequency and are sufficient to promote oscillatory bending of the microbeam. However, while a resonant peak has been previously observed at 930 Hz for a  $690 \times 45 \times 12 \mu m^3$  conducting IPN microbeam [9], the resonance peak of this microactuator would be around 11 kHz [15], above what could be electrically applied and mechanically measured with our experimental setup.



## 4. CONCLUSION

This paper reports on the fabrication of the smallest air-operating microbeam actuator based on conducting polymer. This result was obtained by the synthesis of ultrathin solid polymer electrolyte using a spin coating technique. The solid polymer electrolyte was prepared with an IPN architecture and was synthesized from poly(ethylene oxide) (PEO) and nitrile butadiene rubber (NBR) networks. The combination of ionic conductivity of the PEO partner along with the mechanical properties of NBR network led to flexible SPE as thin as 3.5 $\mu\text{m}$ , suitable with microsystem processes. In a second step, the conducting IPN actuator was prepared by oxidative polymerization of 3,4-ethylenedioxythiophene (EDOT) inside the SPE in order to insure inhomogeneous dispersion of PEDOT throughout the PEO/NBR thickness. To micro-size these materials dry etching was used and led to microbeam actuator as small as 160x30x3.5 $\mu\text{m}^3$ . After incorporating an ionic liquid as electrolyte, the swollen microbeam (160x30x6 $\mu\text{m}^3$ ) was stimulated under square wave potential of +/- 2V. Actuation was demonstrated up to 500 Hz indicating that ionic motions are still present in the membrane at such frequency and can induce oscillatory bending movement of this soft ionic microactuator.

## REFERENCES

- [1] M.-A. De Paoli, Conductive polymer blends and composites, in: H.S. Nalwa (Ed), Handbook of Organic Conductive Molecules and Polymers, Conductive Polymers: Synthesis and Electrochemical Properties, Vol. 2, Chichester: J. Wiley, p. 773 (1997)
- [2] Baughman, R. H., "Conducting Polymer Artificial Muscles" *Synth. Met.* 78 (3) , 339-353 (1996)
- [3] Smela E., "Conjugated polymer actuators for biomedical applications" *Adv. Mater.* 15 (6), 481-494 (2003)
- [4] Otero T. F., Cortes M. T., "Artificial muscles with tactile sensitivity" *Adv. Mater.* 15 (4) 279-282 (2003)
- [5] Ding J, Liu L, Spinks G M, Zhou D, Wallace G G, "High performance conducting polymer actuators utilizing a tubular geometry and helical wire interconnects", *Synth. Met.* 138 (3) 391-398 (2003)
- [6] T. Mirfakhrai, J. D. W. Madden, R. H. Baughman, "Polymer Artificial Muscles" *Mater. Today* **2007**, 10, 30.
- [7] G. Alici, V. Devaud, P. Renaud, G. Spinks, "Conducting polymer microactuators operating in air" *J. Micromechanics Microengineering* 2009, 19, 025017
- [8] A. Khaldi, C. Plesse, C. Soyer, E. Cattan, F. Vidal, C. Legrand, D. Teyssié, "Conducting interpenetrating polymer network sized to fabricate microactuators" *Appl. Phys. Lett.* 2011, 98, 164101
- [9] A. Maziz, C. Plesse, C. Soyer, C. Chevrot, D. Teyssié, E. Cattan, F. Vidal, "Demonstrating kHz Frequency Actuation for Conducting Polymer Microactuators" *Advanced Functional Materials* 2014, 24, 4851
- [10] N. Festin, A. Maziz, C. Plesse, D. Teyssié, C. Chevrot, F. Vidal "Robust solid polymer electrolyte for conducting IPN actuators" *Smart Mater. Struct.* 2013 22 104005
- [11] N. Festin, C. Plesse, P. Pirim, C. Chevrot, F. Vidal, "Electro-active Interpenetrating Polymer Networks actuators and strain sensors. Fabrication, position control and sensing properties" *Sensors Actuators B Chem.* 2014, 193, 82
- [12] T. Sugino, K. Kiyohara, I. Takeuchi, K. Mukai, K. Asaka, "Actuator properties of the complexes composed by carbon nanotube and ionic liquid: The effects of additives" *Sensors Actuators B Chem.* 2009, 141, 179
- [13] Plesse C, Vidal F, Gauthier C, Pelletier J M, Chevrot C, Teyssie D, "Poly(ethylene oxide)/polybutadiene based IPNs synthesis and characterization" *Polymer* 48 (26) 696-703 (2007)
- [14] Vidal F, Plesse C, Teyssié D, Chevrot C, "Long-life air working conducting semi-IPN/ionic liquid based actuator" *Synth. Met.* 142 (1-3) 287-91 (2004)
- [15] Robert D. Blevin, "Formulas for natural frequency and mode shape", Van Nostra, New York, USA, 1978; p. 108